CHEMISTRY
A EUROPEAN JOURNAL

DOI: 10.1002/chem.200700650

Chirally Modified Platinum Generated by Adsorption of Cinchonidine Ether Derivatives: Towards Uncovering the Chiral Sites

Norberto Bonalumi, Angelo Vargas, Davide Ferri, and Alfons Baiker*[a]

Abstract: The adsorption behavior of *O*-methyl and *O*-trimethylsilyl derivatives of cinchonidine (CD), employed as chiral modifiers for heterogeneous enantioselective hydrogenations on supported Pt catalysts, has been investigated by using attenuated total reflection infrared spectroscopy (ATR-IR) and density functional theory (DFT) electronic structure calculations. The ATR-IR spectroscopic investigation provided detailed insight of the adsorbed modifiers under conditions close to those employed during catalytic processes, and electronic structure calculations were used as a complement to the experiments to uncover the implications of conformational changes in generating the topology of the surface chiral site. The structural investigation of the adsorbed modifiers revealed a relationship between the spatial positions of the ether substituents and the enantiodifferentiation induced by the modified catalyst observed in the hydrogenation of α-activated ketones. Experiments and calculations corroborate a model, according to which the addition of a bulky ether group to CD reshapes the chiral sites, thus generating catalytic chiral surfaces with different and, in some cases (e.g. hydrogenation of ketopantolactone), even opposite enantioselective properties to those obtained with CD without altering the absolute configuration of the modifier. The study also confirms that active surface conformations of cinchona modifiers are markedly different from those existing in vacuum and in solution, thus underlying the necessity of investigating the surface-modifier interaction in order to understand enantioselectivity.

Keywords: chiral surfaces · density functional calculations · heterogeneous catalysis · IR spectroscopy · platinum

Introduction

The development of efficient enantioselective catalysts represents an attractive field of research in fine chemical synthesis.[1] While homogeneous enantioselective catalytic hydrogenations have been successfully implemented as a powerful tool in organic synthesis,[2] a corresponding development has not been witnessed in heterogeneous enantioselective catalysis so far, in spite of the technical advantages (stability, regeneration, reuse, and separation) of heterogeneous catalysts compared to their homogeneous counterparts. Nevertheless, in the past decade, considerable efforts have been made by various groups to further develop heterogeneous enantioselective hydrogenations, and today, a significant level of understanding of their functioning has been reached. The most successful strategy for obtaining enantioselective solid catalysts has been the modification of metals by means of chiral organic molecules,[1f,h] albeit control of enantioselectivity induced by such materials has not been reached to the same extent as for homogeneous catalysts.[1b,2] The most studied systems include the enantioselective hydrogenation of β-keto esters with a tartaric-modified nickel catalyst[3,4] and the enantioselective hydrogenation of α-activated ketones[1,5–7] and activated C=C bonds by cinchona-modified Pt and Pd,[8–11] respectively.

It is generally accepted that chiral modification of metal catalysts occurs by adsorption of a chiral molecule on a metal surface, thus generating catalytic sites that can asymmetrically interact with a prochiral substrate.[1f] The sum of such interactions within these sites determines the chiral recognition that is at the origin of enantiodifferentiation. In the case of cinchona-modified platinum, the intrinsic hydrogenation rate is often enhanced (ligand acceleration) and a differential rate enhancement of hydrogenation of one chiral reaction pathway is believed to lead to kinetic resolution.[12,13] For this catalytic system, the structure of the modifier has been thoroughly investigated and the function of

[a] N. Bonalumi, Dr. A. Vargas, Dr. D. Ferri, Prof. A. Baiker
Department of Chemistry and Applied Biosciences
Institute for Chemical and Bioengineering, ETH Zurich
Hönggerberg, 8093, Zurich (Switzerland)
Fax: (+41) 44-632-11-63
E-mail: baiker@chem.ethz.ch

the alkaloid subunits has been identified to a significant extent. A cinchona modifier is characterized by: 1) an anchoring moiety (quinoline ring) that binds the molecule to the surface, 2) stereogenic centers at C8 and C9 that impart asymmetry to the environment, and 3) a basic nitrogen atom (tertiary amine of the quinuclidine moiety) responsible for hydrogen bonding with the substrate at the chiral site.[14] The main characteristics of the corresponding 1:1 modifier–substrate interaction model for the system cinchonidine–ketopantolactone are illustrated in Scheme 1.[15]

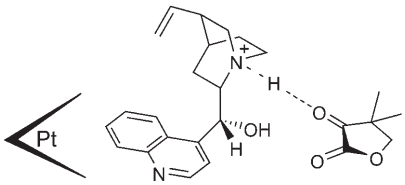

Scheme 1. Simplified model proposed for the interaction between ketopantolactone and cinchonidine adsorbed on the platinum surface.[14,15] A 1:1 diastereomeric complex is formed by hydrogen bonding between the quinuclidine N atom and the carbonyl O atom of ketopantolactone.

The direction of enantioselectivity induced by the modifiers can be controlled to a certain extent. Orito has already observed that in the enantioselective hydrogenation of ethyl pyruvate cinchonidine (CD) yields the *R* lactate, while its diastereomer cinchonine (CN) yields the *S* lactate in almost equal (although not identical) enantiomeric excess.[16] A similar behavior is also observed with the diastereomeric couple quinidine and quinine.[16,17] In the cases described above, the inversion of enantioselectivity is due to the opposite absolute configuration at the C8 and C9 stereogenic centers (Scheme 2). In fact, the diastereomeric couples cinchonidine–cinchonine and quinidine–quinine are often called pseudo-enantiomeric pairs due to their almost enantiomeric structure, which is in line with their behavior as modifiers. More interestingly, it has been shown that inversion of enantioselectivity can be obtained by using modifiers that maintain the same absolute configuration at C8 and C9, but differ by the introduction of an ether moiety in place of the hydroxyl group of CD.[18] In particular, *O*-phenyl ethers of cinchonidine have been shown to yield the *S* enantiomer in the enantioselective hydrogenation of several α-keto esters, as opposed to simple CD that always yields the *R* enantiomer.[18,19] The use of *O*-phenyl cinchonidine (PhOCD) as a modifier showed that the opposite absolute configuration at C8 and C9 of the alkaloid is not a requirement for obtaining inversion of the enantioselective properties of a catalyst. Structural studies of the surface sites generated by this modifier on model metal catalysts revealed that inversion is likely to be attributed to the reshaping of the chiral site due to the phenyl moiety.[20–22] The phenyl group has a complex interaction with platinum, since it can adsorb on the symmetry plane by means of the π system, giving rise to strong chemisorption,[23] therefore influencing the adsorption of the modifier. However, at the same time,

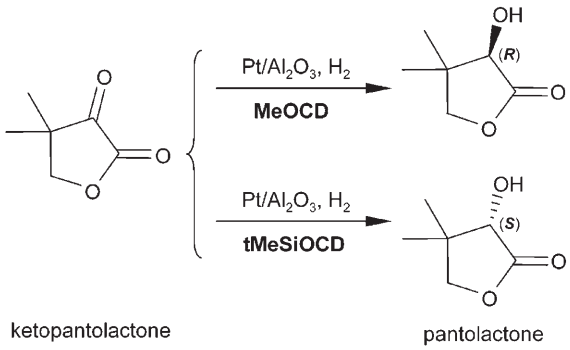

Modifier	R	Chemical structure
CD	H	
MeOCD	–CH_3	
tMeSiOCD		

Scheme 2. Top: Pt-catalyzed enantioselective hydrogenation of ketopantolactone in which chiral modification with MeOCD and tMeSiOCD afford opposite enantiomers of pantolactone.[18] Bottom: Complete chemical structure of CD and its analogues modifiers MeOCD and tMeSiOCD.

it can generate steric repulsion in the proximity of the chiral site. The studies on *O*-phenyl ethers of CD proposed that the reshaping of the asymmetric environment created on the metal catalyst by conformational displacement of the *O*-phenyl moiety is at the origin of the inversion of enantioselective properties with respect to CD.[20–22]

Recently, we showed that the modifiers *O*-methyl cinchonidine (MeOCD) and *O*-trimethylsilyl cinchonidine (tMeSiOCD) (Scheme 2) afford opposite enantioselectivity in the Pt-catalyzed hydrogenation of ketopantolactone. MeOCD affords the *R* enantiomer, and tMeSiOCD the *S* enantiomer with appreciable enantiomeric excess.[18] Here, we apply attenuated total reflection infrared (ATR-IR) spectroscopy and density functional theory (DFT) to elucidate the role of the O–R subunits at C9 of the substituted CD modifiers on the structure of the chiral site. This information is a prerequisite for gaining a thorough understanding of the enantiodifferentiating properties of these catalytic systems.

Results and Discussion

Transmission IR spectra of MeOCD and tMeSiOCD: The transmission IR spectra of neat tMeSiOCD and of solutions of MeOCD and tMeSiOCD in CH_2Cl_2 were used as a refer-

ence for the assignment of the signals of the adsorbed modifiers on Pt (Figure 1). In addition, the vibrational normal modes of tMeSiOCD in its most stable conformation in vacuum (open(3); O(3)) were calculated. The most relevant experimental and calculated vibrational frequencies are reported in Table 1.

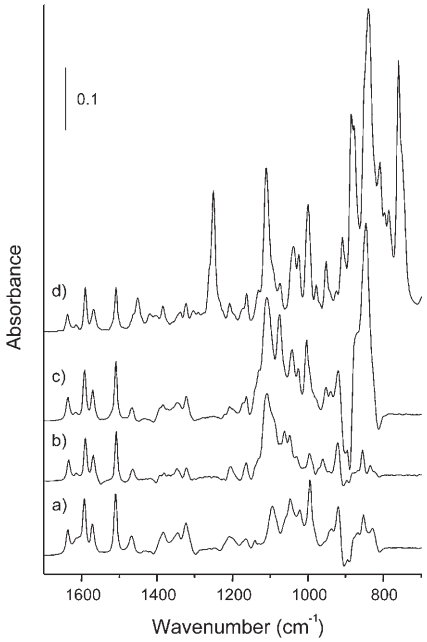

Figure 1. IR transmission spectra of 10 mM CH_2Cl_2 solution of a) cinchonidine (CD), b) *O*-methoxycinchonidine (MeOCD), and c) *O*-trimethylsilyloxycinchonidine (tMeSiOCD). d) Spectrum of neat tMeSiOCD.

Table 1. Assignment of major vibrational modes of tMeSiOCD in solution on Pt/Al_2O_3, and calculated (conformers O(3) in vacuum, see theoretical calculations for details).

MeOCD[a]		tMeSiOCD[a]			
Vibrational frequencies [cm^{-1}]					description of the
sol[b]	Pt[c]	sol[b]	Pt[c]	calcd[d]	vibrational mode[f]
1637	n.o.	1637	n.o.	1654	(C_{10}-C_{11}), ν(C=C)
1613	1613	1613	1613	1604	QN, ring def. + δ(C-H)
1590	1590	1590	1590	1581	QN, ring def. + δ(C-H)
1570	1570	1570	1570	1556	QN, ring def. + δ(C-H)
n.o.	1530	n.o.	1530	n.o.	QN, ring def. + δ(C-H)
1510	1510	1510	1510	1496	QN, ring def. + δ(C-H)
1465	≈1460	1465	≈1450	1464	QD, δ_{as}(C-H)
1465	≈1460	1465	≈1450	1449	QD, δ_{as}(C-H)
		1465	≈1450	1437	QD, δ_{as}(C-H)
		1452[e]	1452	1432	tMe, δ_{as}(CH_3)
				1424	tMe, δ_{as}(CH_3)
				1415	tMe, δ_{as}(CH_3)
		1262[e]	*	1273	tMe, δ_s(CH_3)
		1250	*	1264	tMe, δ_s(CH_3)
			*	1263	tMe, δ_s(CH_3)
1108	n.o.				ν(C-O-CH_3)
		1100	n.o.	1083	ν(C-O) + QD, ρ(CH_2) + ν(Si-O)
		1075	n.o.	1050	QD, ρ(CH_2) + def. C-C
1047	1031	1039	1031	1022	QD, C-N-C, C-C-C, str.
1026	1031	1024	1031	1007	QD, C-N-C, C-C-C, str.
		884	881	880	ν(Si-O) + QD, ρ(CH_3)

[a] For adsorbed MeOCD and tMeSiOCD. [b] IR spectrum of 0.01 M solution in CH_2Cl_2. [c] ATR-IR spectra of 0.05 mM solution in CH_2Cl_2 on Pt/Al_2O_3. [d] DFT calculations performed using the B3LYP method with the 6–31G(d-p) basis set (see text for details), a correlation factor of 0.961 must be taken into account. [e] IR spectrum of neat tMeSiOCD. [f] Vibrational mode description using the following notation: QN = quinoline group; QD = quinuclidine group; tMe = *O*-trimethylsilyl group; ν = stretching; δ_s = symmetric bending; δ_{as} = asymmetric bending; n.o. = not observed; * = interference due to solvent signals.

In the 1650–1450 cm^{-1} spectral range, both modifiers show the common diagnostic vibrational modes of the quinoline ring of CD and its ether derivatives. The signals at 1590, 1570, and 1510 cm^{-1} have already been assigned[24] to a combination of deformation and in-plane δ(C–H) modes of the quinoline ring. The symmetric and asymmetric $\delta(CH_3)$ modes of the trimethylsilyl group lie in the spectral range around 1450 cm^{-1}, partially overlapping with the vibrations of the $\delta(CH_2)$ quinuclidine skeleton (ca. 1460 cm^{-1}). Methyl groups attached to the Si atom have a characteristic, very sharp band between 1290 and 1240 cm^{-1} due to the symmetric ($-CH_3$) deformation, in agreement with previous work on methoxytrimethylsilane.[25,26] For tMeSiOCD, this signal is detected only in the spectrum of the neat compound at 1250 cm^{-1} (Figure 1d), because in solution (Figure 1c) this band is covered by the absorption of the bulk solvent.

Below the 1200 cm^{-1} frequency region, tMeSiOCD exhibits its fingerprint vibrational modes characteristic of asymmetric stretching of Si–O–C, C–C, and C–N groups.[25] The signal at 1100 cm^{-1} is associated with a combination of the ν(C–O) of the trimethylsilyl group and rocking and deformation modes of the methylene groups of the quinuclidine skeleton. Another vibrational mode resulting from a combination of the asymmetric bending of the carbon skeleton of quinuclidine exhibits a band at 1075 cm^{-1}. The intensity ratio between the signals at 1100 and 1075 cm^{-1} of neat tMeSiOCD differs from that of the modifier in solution. The spectrum of the neat modifier (Figure 1d) shows a very weak band at 1075 cm^{-1}, while in solution (Figure 1c), the bands have almost the same intensity. A sharp band at 884 cm^{-1} (Figure 1d) represents a combination of the (Si–O) stretching and $\rho(CH_3)$ of the methyl group directly connected to the Si atom.

The main difference between the transmission spectrum of *O*-methylcinchonidine (MeOCD) shown in Figure 1b and the spectrum of CD (Figure 1a) is the signal at 1108 cm^{-1} associated with a ν(C-O-CH_3) of the methoxy group at C9 (Scheme 2).

ATR-IR spectra of MeOCD and tMeSiOCD adsorbed on Pt: The adsorption behavior of CD has been thoroughly investigated by means of ATR-IR spectroscopy on a polycrystalline Pt surface in the presence of H_2 and solvent.[5,24] Three adsorbed species were identified that are characterized by different adsorption energies and orientation of the quinoline moiety. Strongly adsorbed species are characterized by the quinoline ring of CD predominantly parallel to

the surface plane and show a signal at 1570 cm^{-1}. Weakly adsorbed species are characterized by the quinoline ring tilted with respect to the plane of the metal and have been divided into: 1) N-lone-pair-bonded (signals at 1590 and 1510 cm^{-1}) and 2) α-quinolyl species (signal at 1530 cm^{-1}). Flat adsorbed species generally resist desorption, whereas the last two species mostly disappear during rinsing with H_2-saturated CH_2Cl_2. The same technique was also used for studying the adsorption of *O*-phenyl substituted CD.[20,21]

Figure 2 shows the ATR-IR spectra of tMeSiOCD adsorbed on platinum. They reveal a similar orientation of the

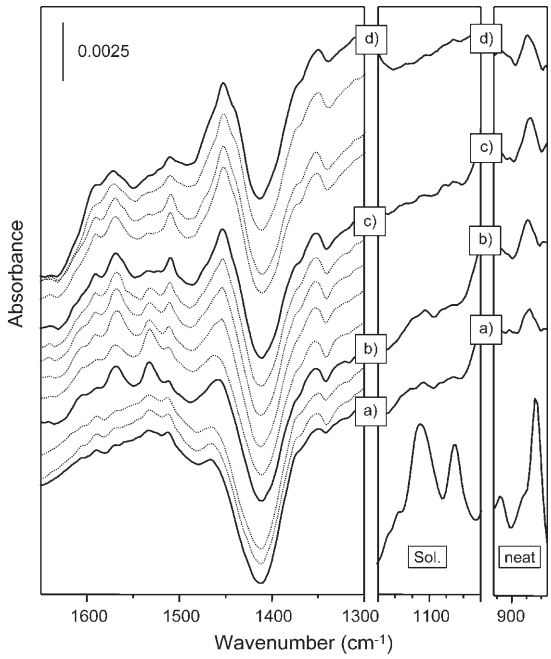

Figure 2. ATR-IR spectra of tMeSiOCD adsorbed from H_2-saturated CH_2Cl_2 on Pt/Al_2O_3 at 293 K (concn tMeSiOCD = 0.05 mM), traces a) and b) were recorded within 10 min. Spectrum c) was recorded after 50 min on stream. Spectrum d) was recorded 40 min after the rinsing of the surface with H_2-saturated CH_2Cl_2. The spectra of tMeSiOCD in solution (Sol.) and neat below 1300 cm^{-1} are included as a reference.

quinoline ring to that of CD with a predominance of strongly adsorbed and α-quinolyl species (Figure 2b). The signal associated with the α-quinolyl adsorbed species decreases with time on stream (Figure 2c), whereas the intensity of the signals at 1590 and 1510 cm^{-1} increases. This is evidence of the reorganization of the population of surface species: when the coverage of tMeSiOCD increases on the surface, α-quinolyl species are replaced by N-lone-pair-bonded species. During rinsing with H_2-saturated CH_2Cl_2, the strongly flat-adsorbed species are the most populated on Pt, while the N-lone-pair-bonded species are slowly displaced from the surface (Figure 2c,d).

The signal at about 1460 cm^{-1} results from a combination of the C–H scissor modes of the quinuclidine skeleton inducing a dynamic dipole moment vector along the N–C4 axis.[24,27] Changes in the intensities of this signal allow the orientation of this sub-unit to be followed. CD and the synthetic modifier *O*-[(3,5-bis(trifluoromethyl)-phenyl]cinchonidine (tFPhOCD) displayed a conformation in which the quinuclidine is oriented directly towards the metal surface.[20] As shown in Figure 2a, in the early stages of the adsorption of tMeSiOCD, the signal associated with the quinuclidine moiety is silent. After 10 min on stream (Figure 2b), a broad band due to the bending mode of the methyl groups connected to the Si atom appears at 1455 cm^{-1}. Although this last band overlaps with the signal of the quinuclidine, a shoulder at approximately 1460 cm^{-1} indicates an orientation of the quinuclidine moiety facing the surface comparable to that of CD.

The signal at 1075 cm^{-1} is associated with a vibrational mode representative of the quinuclidine moiety uncoupled from vibrations originating from other subunits of the modifier, and its dynamic dipole moment is oriented perpendicularly to the N–C4 axis. The absence of this signal in the ATR-IR spectra of the adsorbed tMeSiOCD indicates that the N–C4 axis of quinuclidine is approximately perpendicular to the metal surface, which is corroborated by the presence of the signal at 1460 cm^{-1} discussed in the previous paragraph. In contrast, the signal at 1100 cm^{-1} originates from the combination of vibrational modes of two different sub-units: 1) the ν(C–O) of the Si-O-C group, oriented along the Si–C axis and 2) the rocking of (CH_2) units belonging to the quinuclidine skeleton. The evaluation of the orientation of the Si-O-C group cannot be based on the lack of a signal at 1100 cm^{-1} (Figure 2), since this is affected by the interference (coupling) of the vibrations of the quinuclidine skeleton with the ν(C–O) of the tMeSiO group. This interference changes the direction of the total dynamic dipole moment of the ν(Si-O-C) vibrational mode. Considering that the signal detected at 881 cm^{-1} (Figure 2) is associated with a dynamic dipole moment oriented in the plane of the Si-O-C group, we can assume that the plane of this group is perpendicular to the metal surface.

Figure 3a,b shows the ATR-IR spectra of the evolution of MeOCD adsorbed on platinum. The experiment reveals the presence of mainly two species: the flat 1570 cm^{-1} and the α-quinolyl at 1530 cm^{-1}. Their ratio is constant until the rinsing with solvent (Figure 3c,d) when the intensity of the signal at 1530 cm^{-1} is attenuated. N-lone-pair-bonded species are not detected. These spectroscopic data suggest that the adsorption of MeOCD on Pt is comparable to that of CD.

DFT studies of the surface conformations of adsorbed modifiers: The adsorption of CD and of its phenoxy ether derivatives has been investigated in some detail by means of DFT calculations to help define their conformation on platinum.[20–22,28–31] Figures 4–6 illustrate the calculated conformations of CD, MeOCD, and tMeSiOCD adsorbed on platinum, and Table 2 reports the calculated values of adsorption energies. The peculiarity of the MeO and tMeSiO ether groups as compared to the PhO ether groups analyzed in previous studies[20–22] is that they cannot bind strongly to the metal as a phenyl moiety. Their role is more clearly that of

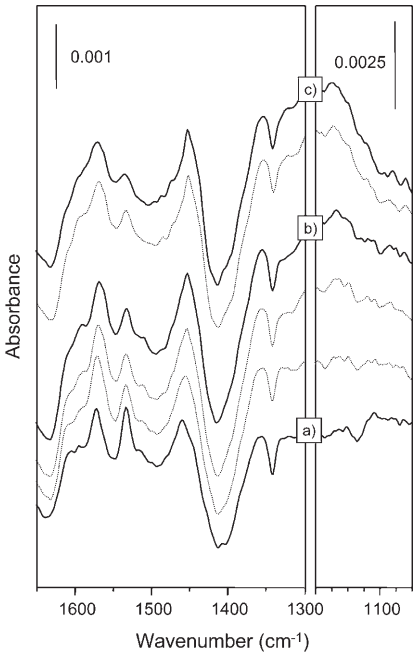

Figure 3. ATR-IR spectra of MeOCD adsorbed from H_2-saturated CH_2Cl_2 on Pt/Al_2O_3 at 293 K (concn MeOCD = 0.05 mM), traces a) and b) were recorded within 60 min. Spectrum c) was recorded 30 min after rinsing the surface with H_2-saturated CH_2Cl_2.

Table 2. Adsorption energies of CD MeOCD and tMeSiOCD (level of theory in the theoretical calculations section). The values are calculated with respect to the O(3) conformation in vacuum for all molecules. All values in kcal mol^{-1}.

	SO(3)	SO(4)	SC(2)	SC(1)	SQB(1)-open	SQB(1)-closed	SQB(2)
CD	42.1	40.6	42.6	43.4	42.79		36.2
MeOCD	34.2	31.8	35.4	34.1	39.0	39.7	
tMeSiOCD			30.8	28.0	36.8	40.0	

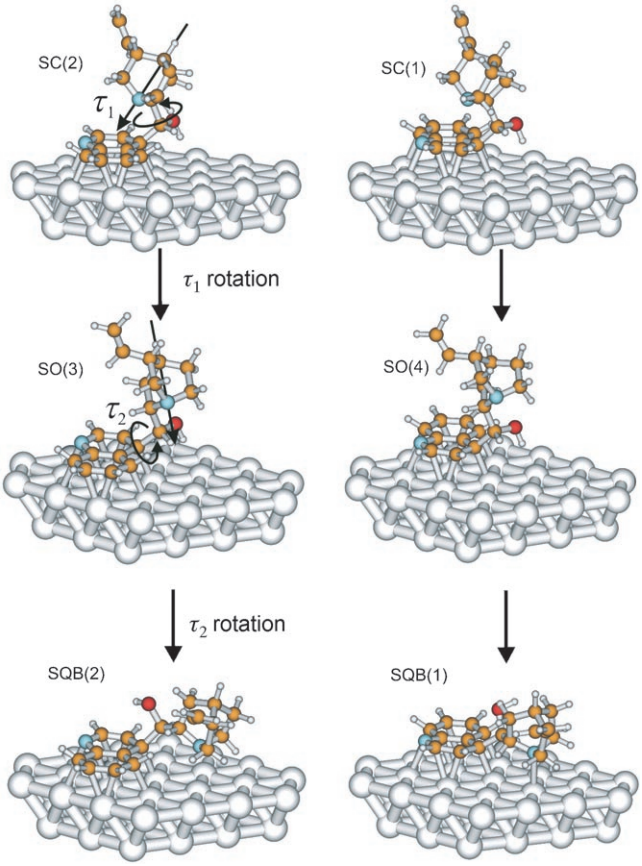

Figure 4. Calculated stable surface conformers of CD on platinum: surface-closed(2) (SC(2)), surface-closed(1) (SC(1)), surface-open(3) (SO(3)), surface-open(4) (SO(4)), surface-quinuclidine-bound(2) (SQB(2)), and surface-quinuclidine-bound(1) (SQB(1)). The straight arrow represents the direction of the N–C4 axis of the quinuclidine ring, and shows the direction of action of the tertiary nitrogen. τ_1 and τ_2 are the rotational degrees of freedom that determine surface conformers. Values of adsorption energies are reported in Table 2.

adding a spatial constraint in the proximity of the chiral site. MeOCD has a small methyl group in place of the hydroxyl group of CD, and tMeSiOCD has a larger trimethylsilyl moiety that is able to increase the van der Waals sphere of the ether group without adding functionalities and may give strong binding to the metal. Furthermore, since the hydroxyl group is replaced by the ether, the role of the hydroxyl group in natural cinchona alkaloids can be assessed further.[19,32]

Figure 4 shows the six stable surface conformations of CD on platinum,[30] and their adsorption energies calculated with respect to the open(3) (O(3)) conformation are reported in Table 2. The designations "open" and "closed" indicate that the quinuclidine nitrogen atom is pointing away (open) or towards (closed) the aromatic quinoline anchoring moiety. With closed conformers, hydrogen-bond interactions with the adsorbed substrate through the quinuclidine nitrogen are hindered. Surface-closed(2) (SC(2)), surface-open(3) (SO(3)), and surface-quinuclidine-bound(2) (SQB(2)) conformations can interconvert by rotation along τ_1 and τ_2 (conformers of the SO(3) group, the left column in Figure 4). Surface-closed(1) (SC(1)), surface-open(4) (SO(4)), and surface-quinuclidine-bound(1) (SQB(1)) can also interconvert by rotation along τ_1 and τ_2 (conformers of the SO(4) group, the right column of Figure 4). Conformers of the two groups cannot interconvert by simple rotation of τ_1 and τ_2, and interconversion requires either a desorption–adsorption step or the rolling of the molecule over the metal surface.[30] The straight arrow depicted along the N–C4 axis of the quinuclidine moieties of SC(2) and SO(3) (Figure 4) represents the range of action of the tertiary nitrogen atom. In SC(2) the nitrogen atom points towards the anchoring group, while in SO(3) it points towards the surface and can therefore contribute to a surface reaction. The same holds for SC(1) and SO(4). Note that the values of adsorption energies in Table 2 are slightly different from the ones previously published,[30] which is due to a different position of the vinyl group. This does not alter the relative adsorption energies and the picture that results from their analysis.

Figure 5 shows the same stable conformers (only SQB(2) is not shown) of MeOCD, and Table 2 reports the calculated adsorption energies with respect to the O(3) conformer. In

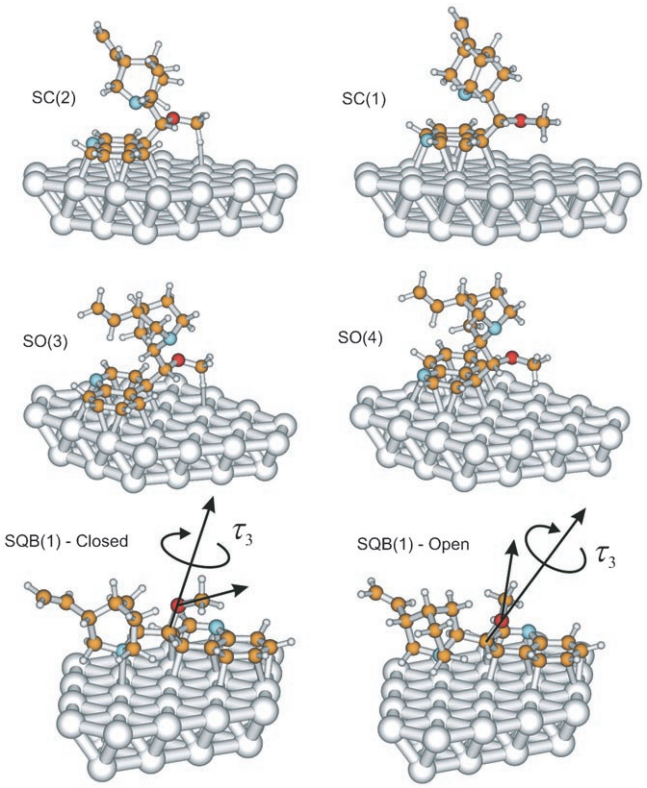

Figure 5. Calculated stable surface conformers of MeOCD on platinum: besides SC(2), SC(1), SO(3), and SO(4), two stable conformers (closed and open) of the surface-quinuclidine-bound(1) (SQB(1)) conformation are illustrated. The position of the *O*-methyl moiety is determined by the rotational degree of freedom τ_3. Values of adsorption energies are reported in Table 2.

the presence of the *O*-methyl moiety, a further rotational degree of freedom is generated, namely τ_3, the rotation of which determines the position in space of the ether moiety. In the closed conformation, the *O*-methyl group occupies a position above the metal and beside the quinuclidine moiety. In the open conformation, it occupies a space opposite the same moiety and above the anchoring group.

Figure 6 shows the SC(2), SC(1), and SQB(1) conformers of tMeSiOCD on platinum, and Table 2 reports the adsorption energies calculated with respect to the O(3) conformer and for the previous modifiers. For this molecule, the SO(3) and SO(4) are not stable and slip to the SC(2) and SC(1) conformations, respectively. This is due to the repulsion of the trimethylsilyl group that destabilizes the surface open conformations. Also, in this case, the τ_3 degree of freedom exists and can generate an open and a closed conformation of SQB(1).

Of all the examined modifiers, the SC(1) and SC(2) conformers have the wrong quinuclidine tertiary nitrogen position (above the anchoring group) to promote surface catalysis. It has, in fact, been shown[29] that the surface-open conformations can bend towards the metal and interact with surface hydrogen. Only from such conformations can the alkaloid interact with surface-bound substrates and generate an enantioselective reaction pathway. On the other hand, surface-quinuclidine-bound conformations are more stable than open conformations. In particular, SQB(1) is more stable than SQB(2).[30] Further evidence towards the hypothesis that conformers of the SO(4) group dominate on the surface is given by the analysis of hydrogenation products of CD,[33] which shows that the absolute configuration of the C(4′) carbon atom (Scheme 2) generated by the partial saturation of a quinoline ring is mostly C4′-(*S*) and can only occur from adsorption in one of the SO(4) group modes.

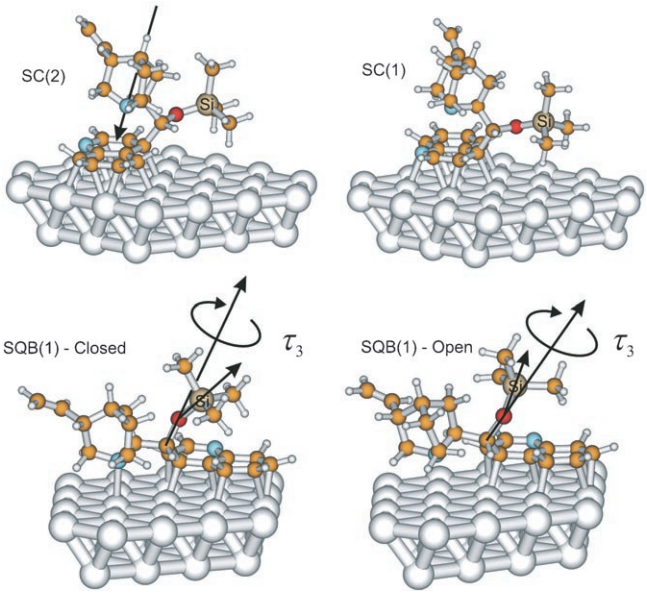

Figure 6. Calculated stable surface conformers of tMeSiOCD on platinum: besides SC(2) and SC(1), two stable conformers (closed and open) of the surface-quinuclidine-bound(1) (SQB(1)) conformation are illustrated. SO(3) and SO(4) conformers are not stable and slip to SC(2) and SC(1), respectively. The position of the tMeSiO moiety is determined by the rotational degree of freedom τ_3. Values of adsorption energies are reported in Table 2.

From Table 2 it emerges that increasing the bulkiness of the ether substituent leads to an increase in the energy difference between the SQB conformations and the surface-open and -closed conformations. In fact, in the case of CD, all surface conformations have comparable values of adsorption energies. For MeOCD, the SQB conformations increase their relative stability compared to surface-open and surface-closed conformers. In the case of tMeSiOCD, this difference is further enhanced. The first important conclusion is indeed that the absence of the hydroxyl group destabilizes surface-open and -closed conformers and that such destabilization increases with the bulkiness of the substituent. Furthermore, within the SQB(1) conformation of tMeSiOCD, the closed conformation of the tMeSiO moiety is more stable than the open one (Figure 6).

Agreement between computed structures and infrared spectra: The preceding results coupled with the spectroscopic data shown in the previous paragraph suggest that cinchona alkaloids adsorbed on a metal surface do not adopt surface-open or surface-closed conformers when the quinuclidine tertiary nitrogen atom is relatively far from the metal. However, they are more likely to adopt conformations where the quinuclidine moiety is close or attached to the metal. The ATR-IR experiments show a very similar behavior of the three alkaloids concerning the main adsorption features, indicating that similar chiral sites are formed at the solid–liquid interface. Analyzing the catalytic experiments, it emerges that CD has a similar behavior to MeOCD (the same enantiomer is formed in the hydrogenation of α-activated ketones). This excludes the hydroxyl group from having a critical role in the chiral recognition, at least for the examined class of substrates. On the other hand, in the same reactions, tMeSiOCD affords either a lower *ee* or an excess in the opposite enantiomer as observed for ketopantolactone hydrogenation (see Table 1 in reference [18]). This behavior could originate from the reshaping of the chiral space due to its large van der Waals radius. When considering the adsorption of this modifier, the surface-open and -closed conformers (Figure 6) are very unlikely to participate in the enantioselective event, since their fractional coverage should be very low. In fact, surface-open conformers are not even predicted to be stable. It should be noted that if these last conformers did have a role in enantioselectivity, this modifier should not give an enantiomeric excess. This constitutes strong evidence in favor of the predominant role of chiral sites of the SQB type in which the quinuclidine tertiary nitrogen atom is closer to the metal.

From previous analysis, it emerged that the dimension of the van der Waals sphere of the ether group is critical in inverting the preferred docking of the substrate. The small methyl group leaves the chiral site almost unaltered leading to a very similar enantioselectivity to that generated by CD, but in the hydrogenation of α-activated ketones the larger trimethylsilyl group redefines the docking space leading to the opposite, the *S* enantiomer in the case of the hydrogenation of the ketopantolactone.[18] Importantly, the most stable SQB(1) conformation is when the trimethylsilyl group is within the chiral site (SQB(1) closed, Figure 6). The SQB(1) open conformation has a chiral site comparable to that of CD and MeOCD, but this conformer is 3 kcal mol^{-1} less stable than the SQB(1) closed one, leading to the mentioned reshaping of the chiral site.

For clarity, the interaction model used is the one mentioned in the introduction (Scheme 1), in which the quinuclidine nitrogen atom interacts through a hydrogen bond to the keto-carbonyl group of the substrate.[15,34] This evidently requires that the tertiary nitrogen atom is detached from the surface. The process of hydrogen uptake by means of a quinuclidine moiety of CD on a hydrogen-rich platinum surface has been previously shown by means of theoretical calculations[29] and is corroborated by experimental observations.[35,36]

Other proposals within the 1:1 interaction model have been made. According to Augustine,[37] the interaction between the tertiary amine and the keto-carbonyl moiety of the substrate occurs by means of a nucleophilic attack of the nitrogen to C=O, but this proposal also involves the participation of the hydroxyl moiety of CD, which cannot help to interpret the behavior of CD ethers where the OH is absent. Furthermore, in this model, the O(3) conformation of adsorbed CD is postulated. This also does not fit with the present results for the CD ethers. This model has been revisited by Vayner et al., who proposed a zwitterionic intermediate formed between the quinuclidine nitrogen and the keto-carbonyl moiety of the substrate, but without the participation of the hydroxyl group of CD.[38] Although there is no experimental evidence for the formation of such a zwitterionic intermediate,[39] it is useful to note that, according to this interaction model, the chiral site would be critically influenced by the bulkiness of the trimethylsilyl group. However, the authors also postulate a chiral site formed by the O(3) conformation of the alkaloid on the metal (SO(3)), which has been shown to be unlikely for CD ethers. The surface structures proposed in this contribution represent an interesting challenge for another interpretation of enantioselectivity recently proposed and based on the interaction of the prochiral activated ketone with both the quinuclidine tertiary nitrogen and the aromatic hydrogen atoms of the anchoring moiety. According to this model,[40] a two-point interaction could stir enantioselectivity: quinuclidine nitrogen and aromatic hydrogen atoms would be the binding points in the chiral site. Support for this view is provided by ultra-high vacuum (UHV) studies of the interactions between adsorbed aromatic molecules and esters which show that, under the experimental conditions used, for example on a metal–vacuum interface, such interactions indeed occur and can be observed.[41] The resulting interaction model postulates an O(3) conformation of adsorbed CD, which we have shown to be unlikely. Still it could be argued that hydrogen-bonding interactions between substrate and anchoring group could also occur for the SQB(1) adsorption mode of the modifier, but a closer inspection of the SQB(1) structure of tMeSiOCD indicates that the presence of the trimethylsilyl moiety rules out a two points interaction, since it blocks the access to the aromatic hydrogen atoms of the anchoring moiety.

Conclusion

Understanding the nature of the chiral sites obtained by adsorption of conformationally complex chiral modifiers to platinum is of critical importance for the interpretation of enantioselectivity. ATR-IR spectroscopy has been used to obtain detailed information on the structure of the solid–liquid interface formed by adsorption of MeOCD and tMeSiOCD on a model platinum catalyst under conditions close to those of the real catalyst. This analysis has revealed that the main adsorption features of the adsorbed molecules cor-

respond to those observed in previous studies for CD with the important difference that, for tMeSiOCD, the trimethylsilyl moiety is positioned within the chiral site in a conformation that allows the detection of the vibrational normal modes with a component of the dynamic dipole moment perpendicular to the plane of the surface. Electronic structure calculations of the adsorption structures of MeOCD and tMeSiOCD with respect to the same calculations for unsubstituted CD help to understand the topology of the chiral site and corroborate the spectroscopic results. CD ethers enhance their preference, as already shown for CD, for conformations in which the quinuclidine nitrogen is close to the metal. In particular, for tMeSiOCD, no energy minimum is found corresponding to surface-open conformers due to the steric repulsion of the tMeSiO substituent. Thus, a model is proposed according to which the steric interference within the chiral site (formed by the structure of the adsorbed alkaloid) allows inversion of the docking preference, thus explaining the opposite enantioselectivity observed with the use of MeOCD and tMeSiOCD in the hydrogenation of ketopantolactone. The key concept at the origin of chiral recognition is the accessibility to the chiral site. Fine tuning of the chiral site can be obtained by the introduction of sterically hindering substituent groups that change the topology of the chiral site. We anticipate that these findings trigger a further level of understanding of asymmetric catalytic surfaces generated by the strong adsorption of chiral molecules to a catalytically active metal.

Experimental Section

Materials: *O*-Methylcinchonidine (MeOCD, Ubichem, >99.5) and *O*-trimethylsilylcinchonidine (tMeSiOCD, Ubichem, >98.5%) were used as received. Dichloromethane (Baker, technical grade) was stored over 5 Å molecular sieves. N_2 (99.995 vol%) and H_2 (99.999 vol%) gases were supplied by PANGAS.

Film preparation: The Pt/Al_2O_3 thin films used for ATR-IR spectroscopy were prepared on a trapezoidal germanium internal reflection element (IRE, $50\times20\times1$ mm^3) by electron beam vapor deposition. Pt and Al_2O_3 targets were heated with an electron beam as described in detail elsewhere.[42] First, 50 nm of Al_2O_3 were deposited followed by 1 nm of Pt.

IR and ATR-IR spectroscopy: The infrared spectrum of the pure modifier was recorded with a MVP ATR unit (Zn-Se crystal, Harrick) and an IFS-66/S spectrometer (Bruker Optics). In situ ATR-IR spectra were recorded on the same spectrometer equipped with a commercial ATR accessory (Optispec) and a liquid-nitrogen-cooled MCT detector. Spectra were collected by co-adding 200 scans at 4 cm^{-1} resolution. After cell-mounting and optic-alignment, the probe chamber was purged overnight with N_2 gas. The assembled stainless steel flow-through cell was maintained at 293 K throughout the experiments. N_2-saturated CH_2Cl_2 was circulated over the thin film at 1.0 mL min^{-1} for about 45 min using a peristaltic pump until achievement of steady-state conditions under which the infrared spectra did not change significantly. Before adsorption, the Pt film was treated with H_2-saturated solvent for about 3 min. A H_2-saturated solution of the modifier under investigation at the desired concentration was then admitted to the cell for about one hour followed by rinsing with H_2-saturated solvent to remove weakly adsorbed and dissolved species. All spectra are presented in absorbance units and, where needed, signals from atmospheric water were subtracted in the 1700–1400 cm^{-1} range. Spectra of CH_2Cl_2 solutions and neat liquids were obtained in the transmission mode (200 scans, 4 cm^{-1} resolution).

Theoretical calculations: Normal mode analyses were performed with the Gaussian98 set of programs,[43] with the density functional theory formalism with a B3LYP Hamiltonian[44,45] and a 6–31G (d–p) basis set.[46] Adsorption studies were performed using the Amsterdam Density Functional (ADF) program package.[47] The surface was simulated by using a Pt_{38} cluster as described in detail elsewhere.[30,31] A frozen core approximation was used for the description of the inner core of the atoms. Orbitals up to 1s were kept frozen for the second-row elements, and orbitals up to 4f were kept frozen for platinum. Decreasing the Pt frozen core to 4d, implying the explicit calculation of 14 additional electrons per platinum atom, has been shown to increase the adsorption energy by only about 5 kJ mol^{-1} for the adsorption of benzene.[48] The importance of relativistic effects has been shown for calculations involving platinum;[49,50] therefore, the core was modeled by using a relativistically corrected core potential created with the DIRAC utility of the ADF program. The DIRAC calculations implied the local density functional in its simple X-α approximation without any gradient correction, but the fully relativistic Hamiltonian was used, including spin-orbit coupling. Furthermore, the relativistic scalar approximation (mass-velocity and Darwin corrections) was used for the Hamiltonian with the zero-order regular approximation (ZORA) formalism,[51] in which spin-orbit coupling is already included in the zero order. The ZORA formalism requires a special basis set to include much steeper core like functions implemented in the code. Within this basis set, the double-ζ (DZ) basis functions were used for platinum. For second-row elements and hydrogen, double-ζ polarized (DZP) basis functions were used.[52] The local part of the exchange and correlation functional was modeled by using a Vosko, Wilk, Nuisar parameterization of the electron gas.[53] The nonlocal part of the functional was modeled using the Becke correction for the exchange[54] and the Perdew correction for the correlation.[55] All calculations were run unrestricted.

Catalytic tests: Catalytic tests were performed using a parallel pressure reactor system (Endeavour, Argonaut Technologies).[18] Conditions: pre-reduced 5 wt% Pt/Al_2O_3 (Engelhard, type 4759; 42 mg), substrate (1.84 mmol) and modifier (6.8 μmol) in THF (5 mL), room temperature at 1 bar H_2 pressure for 2 h.

Acknowledgements

The authors gratefully acknowledge the financial support by the Swiss National Science Foundation, the Foundation Claude and Giuliana, and the Swiss Center for Scientific Computing (Manno) for computational resources.

[1] a) M. Heitbaum, F. Glorius, I. Escher, *Angew. Chem.* **2006**, *118*, 4850; *Angew. Chem. Int. Ed.* **2006**, *45*, 4732–4762; b) H. U. Blaser, B. Pugin, F. Spindler, *J. Mol. Catal. A* **2005**, *231*, 1–20; c) G. J. Hutchings, *Annu. Rev. Mater. Sci.* **2005**, *35*, 143–166; d) A. Baiker, *Catal. Today* **2005**, *100*, 159–170; e) D. Y. Murzin, P. Mäki-Arvela, E. Toukoniitty, T. Salmi, *Catal. Rev. Sci. Eng.* **2005**, *47*, 175–256; f) A. Baiker, H.-U. Blaser, *Handbook of Heterogeneous Catalysis* (Eds.: G. Ertl, H. Knözinger, J. Weitkamp), Wiley-VCH, Weinheim (Germany), **1997**, p. 2422; g) M. Bartók, *Curr. Org. Chem.* **2006**, *10*, 1533–1567; h) A. Baiker, *Curr. Opin. Solid State Mater. Sci.* **1998**, *3*, 86.

[2] a) R. Noyori, *Adv. Synth. Catal.* **2003**, *345*, 15; b) H. Becker, K. B. Sharpless, *Asymmetric Oxidation Reactions: A Practical Approach in Chemistry*, Oxford University Press, New York, **2001**; c) W. S. Knowles, *Adv. Synth. Catal.* **2003**, *345*, 3.

[3] T. Sugimura, S. Nakagawa, A. Tai, *Bull. Chem. Soc. Jpn.* **2002**, *75*, 355–363.

[4] T. Osawa, T. Harada, O. Takayashu, *Top. Catal.* **2000**, *13*, 155–168.

[5] T. Bürgi, A. Baiker, *Acc. Chem. Res.* **2004**, *37*, 909–917.

[6] A. Baiker, *J. Mol. Catal. A* **2000**, *163*, 205–220.

[7] M. Studer, H. U. Blaser, C. Exner, *Adv. Synth. Catal.* **2003**, *345*, 45–65.

[8] M. Maris, W. R. Huck, T. Mallat and A. Baiker, *J. Catal.* **2003**, *219*, 52–58.
[9] W. R. Huck, T. Mallat, A. Baiker, *New J. Chem.* **2002**, *26*, 6–8.
[10] W. R. Huck, T. Mallet, A. Baiker, *J. Catal.* **2000**, *193*, 1–4.
[11] A. Tungler, E. Sipos, V. Hada, *Curr Org. Chem.* **2006**, *10*, 1569–1583.
[12] A. Vargas, T. Bürgi, M. von Arx, R. Hes, A. Baiker, *J. Catal.* **2002**, *209*, 489–500.
[13] A. Vargas, T. Bürgi, A. Baiker, *New J. Chem.* **2002**, *26*, 807–810.
[14] A. Baiker, *J. Mol. Catal. A* **1997**, *115*, 473–493.
[15] N. Bonalumi, T. Bürgi, A. Baiker, *J. Am. Chem. Soc.* **2003**, *125*, 13342–13343.
[16] Y. Orito, S. Imai, S. Niwa, *J. Chem. Soc. Jpn.* **1980**, 670–672.
[17] L. Balazs, T. Mallat, A. Baiker, *J. Catal.* **2005**, *233*, 327–332.
[18] S. Diezi, T. Mallat, A. Szabo, A. Baiker, *J. Catal.* **2004**, *228*, 162–173.
[19] S. Diezi, A. Szabo, T. Mallat, A. Baiker, *Tetrahedron: Asymmetry* **2003**, *14*, 2573–2577.
[20] A. Vargas, D. Ferri, N. Bonalumi, T. Mallat, A. Baiker, *Angew. Chem.* **2007**, *119*, 3979; *Angew. Chem. Int. Ed.* **2007**, *46*, 3905.
[21] N. Bonalumi, A. Vargas, D. Ferri, T. Bürgi, T. Mallat, A. Baiker, *J. Am. Chem. Soc.* **2005**, *127*, 8467–8477.
[22] N. Bonalumi, A. Vargas, D. Ferri, A. Baiker, *J. Phys. Chem. C* **2007**, *111*, 9349–9358
[23] N. Bonalumi, A. Vargas, D. Ferri, A. Baiker, *J. Phys. Chem. B* **2006**, *110*, 9956–9965.
[24] D. Ferri, T. Bürgi, *J. Am. Chem. Soc.* **2001**, *123*, 12074–12084.
[25] G. Socrates, *Infrared and Raman Characteristic Group Frequencies*, Wiley, New York, **2001**.
[26] M. Montejo, F. P. Urena, F. Marquez, I. S. Ignatyev, J. L. Gonzalez, *J. Mol. Struct.* **2005**, *744*, 331–338.
[27] W. Chu, R. J. LeBlanc, C. T. Williams, J. Kubota, F. Zaera, *J. Phys. Chem. B* **2003**, *107*, 14365–14373.
[28] A. Vargas, T. Bürgi, A. Baiker, *J. Catal.* **2004**, *226*, 69–82.
[29] A. Vargas, D. Ferri, A. Baiker, *J. Catal.* **2005**, *236*, 1–8.
[30] a) A. Vargas, A. Baiker, *J. Catal.* **2006**, *239*, 220–226; b) A. Vargas, A. Baiker, *J. Catal.* **2007**, *247*, 387.
[31] A. Vargas, A. Baiker, *Mol. Simul.* **2006**, *32*, 1241–1247.
[32] R. Hess, S. Diezi, T. Mallat, A. Baiker, *Tetrahedron: Asymmetry* **2004**, *15*, 251–257.
[33] G. Szollosi, A. Chatterjee, N. Forgo, M. Bartók, F. Mizukami, *J. Phys. Chem. A* **2005**, *109*, 860–868.
[34] O. Schwalm, B. Minder, J. Weber, A. Baiker, *Catal. Lett.* **1994**, *23*, 271–279.
[35] I. C. Lee, R. I. Masel, *J. Phys. Chem. B* **2002**, *106*, 368–373.
[36] I. C. Lee, R. I. Masel, *J. Phys. Chem. B* **2002**, *106*, 3902–3908.
[37] R. L. Augustine, S. K. Tanielyan, L. K. Doyle, *Tetrahedron: Asymmetry* **1993**, *4*, 1803–1827.
[38] G. Vayner, K. N. Houk, Y. K. Sun, *J. Am. Chem. Soc.* **2004**, *126*, 199–203.
[39] E. Orglmeister, T. Mallat, A. Baiker, *J. Catal.* **2005**, *234*, 242–246.
[40] S. Lavoie, M. A. Laliberte, I. Temprano, P. H. McBreen, *J. Am. Chem. Soc.* **2006**, *128*, 7588–7593.
[41] S. Lavoie, G. Mahieu, P. H. McBreen, *Angew. Chem.* **2006**, *118*, 7564; *Angew. Chem. Int. Ed.* **2006**, *45*, 7404–7407.
[42] D. Ferri, T. Bürgi, A. Baiker, *J. Phys. Chem. B* **2001**, *105*, 3187–3195.
[43] Gaussian 98 (Revision A.7), M. J. Frisch, G. W. Trucks, H. B. Schlegel, G. E. Scuseria, M. A. Robb, J. R. Cheeseman, V. G. Zakrzewski, J. A. Montgomery, R. E. Stratmann, J. C. Burant, S. Dapprich, J. M. Millam, A. D. Daniels, K. N. Kudin, M. C. Strain, O. Farkas, J. Tomasi, V. Barone, M. Cossi, R. Cammi, B. Mennucci, C. Pomelli, C. Adamo, S. Clifford, J. Ochterski, G. A. Petersson, P. Y. Ayala, Q. Cui, K. Morokuma, D. K. Malick, A. D. Rabuck, K. Raghavachari, J. B. Foresman, J. Cioslowski, J. V. Ortiz, B. B. Stefanov, G. Liu, A. Liashenko, P. Piskorz, I. Komaromi, R. Gomperts, R. L. Martin, D. J. Fox, T. Keith, M. A. Al-Laham, C. Y. Peng, A. Nanayakkara, C. Gonzalez, M. Challacombe, P. M. W. Gill, B. G. Johnson, W. Chen, M. W. Wong, J. L. Andres, M. Head-Gordon, E. S. Replogle, J. A. Pople, Gaussian, Inc., Pittsburgh, PA, **1998**.
[44] A. D. Becke, *J. Chem. Phys.* **1993**, *98*, 5648–5652.
[45] C. Lee, W. Yang, R. G. Parr, *Phys. Rev. B* **1988**, *37*, 785–789.
[46] P. C. Hariharan, J. A. Pople, *Theor. Chem. Acc.* **1973**, *28*, 213–222.
[47] ADF—Amsterdam Density Functional, E. J. Baerends, J. Autschbach, A. Berces, C. Bo, P. M. Boerrigter, L. Cavallo, D. P. Chong, L. Deng, R. M. Dickson, D. E. Ellis, L. Fan, T. H. Fischer, C. F. Guerra, S. J. A. van Gisbergen, J. A. Groeneveld, O. V. Gritsenko, M. Grönning, F. E. Harris, P. van den Hoek, H. Jacobsen, G. van Kessel, F. Kootstra, E. vanLenthe, V. P. Osinga, S. Patchkovskii, P. H. T. Philipsen, D. Post, C. C. Pye, W. Ravenek, P. Ros, P. R. T. Schipper, G. Schreckenbach, J. G. Snijders, M. Sola, M. Swart, D. Swerhone, G. teVelde, P. Vernooijs, L. Versluis, O. Visser, E. van Wezenbeek, G. Wiesenekker, S. K. Wolff, T. K. Woo, T. Ziegler, in Scientific Computing and Modelling NV, Vrije Universiteit, Theoretical Chemistry, Amsterdam, **2004**.
[48] M. Saeys, M.-F. Reyniers, G. B. Marin, M. Neurock, *J. Phys. Chem. B* **2002**, *106*, 7489–7498.
[49] P. H. T. Philipsen, E. van Lenthe, J. G. Snijders, E. J. Baerends, *Phys. Rev. B* **1997**, *56*, 13556.
[50] G. Pacchioni, S. C. Chung, S. Kruger, N. Rosch, *Surf. Sci.* **1997**, *392*, 173.
[51] E. van Lenthe, E. J. Baerends, J. G. Snijders, *J. Chem. Phys.* **1999**, *110*, 8943.
[52] E. van Lenthe, E. J. Baerends, *J. Comput. Chem.* **2003**, *24*, 1142–1156.
[53] S. H. Vosko, L. Wilk, M. Nusair, *Can. J. Phys.* **1980**, *58*, 1200.
[54] A. D. Becke, *Phys. Rev. A* **1988**, *38*, 3098.
[55] J. P. Perdew, *Phys. Rev. B* **1986**, *33*, 8822–8824.

Received: April 27, 2007
Published online: August 31, 2007

